

Comparison of simulated and actual performance of an optical detector in low temperature

B., Boroomand-Nasab, A., Kavsariyan, and M., Soroosh

Electrical Department of Engineering Faculty, Shahid Chamran University, Ahvaz, Iran,
B-Boroomand@mststu.scu.ir

Abstract: Optoelectronic devices in the range between LWIR and MWIR has applications such as optical gas sensing, free-space optical communications, infrared measurement, thermal imaging and biomedical etc. [1] Expression of applications, the need for research in the simulation of semiconductor detector features felt. HgCdTe semiconductor detector with a narrow band gap, which can range in wavelength of the aforementioned acts. its possible to show an elements behavior and Performance by simulated without making it. So far, extensive research to reduce dark current and rise in device operation temperature is performed. Use at low temperatures will result in increased costs. The aim of this study was to compare the actual and simulated a light detector Hg_{1-x}Cd_xTe by considering tunneling effect, the recombination Auger and SRH. To achieve this goal, assist those equations to simulate drift - diffusion is done in MATLAB software.

[SB., Boroomandnasab , A., Kavsariyan , and M., Soroosh. **Comparison of simulated and actual performance of an optical detector in low temperature.** *Rep Opinion* 2013;5(8):28-31]. (ISSN: 1553-9873).
<http://www.sciencepub.net/report>. 4

Keywords: Optical detector, simulation, drift - diffusion, tunneling, recombination Auger, recombination SRH

1 – Introduction

Infrared detector have been used for four decades. To access the infrared wavelength region of narrow band materials have been investigated. Especially for this purpose, substances II - VI are provided great flexibility, because it can also as a wide band gap material, as well as narrow band gap material act. Properties of narrow-band HgCdTe, make it an important material for infrared detection. With its band gap tunnel leading to new hybrid devices, Also allows HgCdTe to have features of both LWIR and MWIR. Infrared wavelengths are shown in table 1.

table 1: spectral region

Spectral Region	Range
Near Infrared (NIR)	0.78 – 1 μm
Short wavelength IR (SWIR)	1–3 μm
Medium wavelength IR (MWIR)	3–8 μm
Long wavelength IR (LWIR)	8–14 μm
Very long wavelength IR (VLWIR)	14–1000 μm

Despite the potential applications of HgCdTe, there are obstacles in its design and construction, Which to build an efficient detector to overcome them. The most important challenge device performance at low temperatures (liquid nitrogen temperature) to achieve high efficiency.

2 - Numerical Modeling

A one-dimensional model to simulate the drift and diffusion bonded to evaluate the features and performance of HgCdTe optical detector is used.

Relations Fermi - Dirac to calculate the density of electrons and holes within the device is used.

Simulation $P^+ - n$ plot has been shown in Figure 2.

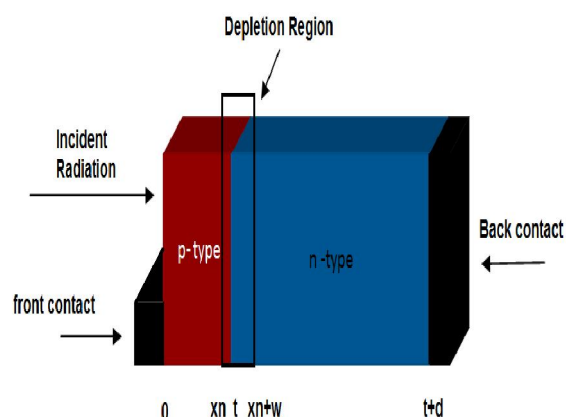


Figure 2

Drift diffusion simulations using a set of transport equations to describe the behavior of the device. Continuity equations for electrons and holes, the Poisson equation and all related recombination mechanisms are used. Poisson's equation for equilibrium is given by Equation 1.

$$\nabla^2 \cdot \varphi = -\frac{q}{\epsilon} (n - p + N_D^+ - N_A^-) \quad (1)$$

Where, N_D^+ and N_A^- are the ionized donor and acceptor concentrations and φ is the electrostatic potential. LU decomposition method for solving the Poisson equation, we have used a uniform mesh. To calculate the current state of conservation, the

continuity equation has been shown by equations 2 and 3 have been resolved.

$$J_n = -q\mu_n n \left(-\frac{d\phi}{dx} \right) + qD_n \frac{dn}{dx} \quad (2)$$

$$J_p = -q\mu_p p \left(-\frac{d\phi}{dx} \right) - qD_p \frac{dp}{dx} \quad (3)$$

where, $J_{n,p}$ is the current density, $\mu_{n,p}$ is the carrier mobility and $D_{n,p}$ is the diffusion coefficient. The diffusion coefficient for degenerate materials cannot simply be determined by the Einstein's relation and is therefore determined by Kroemer's expansion [2].

3 - Theoretical Model

The molar concentration plays an important role in the determination of basic parameters such as band gap, intrinsic carrier concentration, effective mass, mobility and dielectric constant. These parameters are very sensitive to temperature [3].

a) The intrinsic carrier concentration

$$n_i = (5.585 - 3.820x + 1.753 \times 10^{-3}T - 1.364 \times 10^{-3}xT) \times E_g^{3/4} T^{3/2} e^{\left(-\frac{E_g}{2kT} \right)} \quad (4)$$

The "X" cadmium mole fraction, T is the temperature, E_g the band gap.

b) Band gap:

$$E_{(x,T)} = -0.302 + 1.93x + 5.35 \times 10^{-4}T(1 - 2x) - 0.810x^2 + 0.832x^3 \quad (5)$$

c) Effective mass of the electron:

$$m_n^* = \frac{1}{-0.6 + 6.333 \left(\frac{x}{E_g} + \frac{1}{E_g + 4} \right)} \quad (6)$$

Hole mass m_p^* is equal to $0.55 m_0$.

d) Electron and hole mobility

$$\mu_e = 9 \times 10^4 \left(\frac{0.2}{x} \right)^{7.5} T^{-2} \left(\frac{0.2}{x} \right)^{0.25} \quad (7)$$

$$\mu_h = \frac{\mu_e}{100} \quad (8)$$

e) Electric permittivity

$$\epsilon_{HgCdTe} = 20.5 - 15.5x + 5.7x^2 \quad (9)$$

f) Absorption coefficient

two particular characterize the absorption coefficient, the Kane region, which describes the absorption for energies above the conduction band and the Urbach region, which describes the absorption for all energies below the conduction band edge [4].

$$\alpha = \beta \sqrt{E - E_g} \quad (10a)$$

$$\beta = -1 + 0.0837 + (21 - 0.137)x \quad (10b)$$

$$\alpha = \alpha_0 e^{\left(\frac{E - E_g}{T - T_0} \right)} \quad (11a)$$

$$\alpha_0 = 3.267 \times 10^4 (1 + x) \quad (11b)$$

$$E_0 = (1.838x) - 0.3424 \quad (11c)$$

$$T_0 = 81.9 \quad (11d)$$

g) Mechanisms recombination

In this study, the mechanism is considered Auger, SRH and radiant. recombination SRH given by the following equation.

$$R_{SRH} = \frac{pn - n_i^2}{\tau_p \left[n + n_{ie} \left(\frac{E_t - E_i}{kT} \right) \right] + \tau_n \left[p + n_{ie} \left(\frac{E_i - E_t}{kT} \right) \right]} \quad (12)$$

where, ' E_t ' is the trap level, ' E_i ' is the intrinsic Fermi energy and ' $\tau_{n,p}$ ' are the carrier lifetimes.

Radiative recombination is a recombination band to band, Including direct annihilation of a conduction electron band with the hole in the valence band. Additional energy generated, usually in the form of a photon will be free. This mechanism is a direct band gap material. Radiative recombination given by the following equation.

$$R_{Radiative} = B(pn - n_i^2) \quad (13)$$

Where B is given by the following equation.

$$B = (5.8 \times 10^{-13}) \epsilon^{\frac{1}{3}} \left(\frac{m_0}{m_e^* + m_h^*} \right) \left(1 + \frac{m_0}{m_e^*} + \frac{m_0}{m_h^*} \right) \left(\frac{300}{T} \right)^{\frac{3}{2}} (E_g^2 + 3kTE_g + 3.75k^2T^2) \quad (14)$$

Since $Hg_{1-x}Cd_xTe$ is a direct band gap material, Expected to play a major role in Radiative recombination.

Auger recombination is a one of the dominant mechanisms of HgCdTe with narrowband gap.

The Auger generation is Usually the Predominant parameter of dark current at high temperatures, that's why our photodetector Operates at near Liquid nitrogen temperature, But this will increase the operation cost. Auger generation-recombination is given by Equation 15.

$$R_{Auger} = C_n (pn^2 - nn_i^2) + C_p (np^2 - pn_i^2) \quad (15)$$

C_n and C_p are Auger coefficients. Which can be found in reference [5].

h) In the narrow band HgCdTe under reverse bias band to band tunneling is likely to increase with increasing reverse voltage that in approximate WKB [6] it can be formed like Equation 16.

$$G_T(x) = \frac{\sqrt{2}q^2\sqrt{m^*}F_x^2}{4\pi^2\hbar\sqrt{E_g}} \exp\left[-\frac{\pi\sqrt{m^*}E_g^{3/4}}{2\sqrt{2}q\hbar F_x}\right] \quad (16)$$

Where, G_T is expressed as a rate of tunneling and F_x is the local electric field.

i) When balance is trapped in the middle of the band, allowing tunneling to a trap level rises and with a high electric field can expect a large variance of the I-V diagram. The trap assisted tunneling can be expressed as a slight modification of equation 12 by adding a field effect factor 'Γn,p' [7]

$$R_{SRH} = \frac{pn - n_i^2}{\frac{\tau_p}{1+\tau_p} \left[n + n_i e^{\frac{E_T - E_i}{kT}} \right] + \frac{\tau_n}{1+\tau_n} \left[p + n_i e^{\frac{E_i - E_T}{kT}} \right]} \quad (17)$$

j) Dynamic resistance is an increasing resistance, which is measured by the following equation.

$$D^* = \frac{n\lambda q}{hc} \left[\frac{4kT}{R_{opt}A} + 2q^2\eta P_{OPT} \right]^{-2} \quad (18)$$

4 – Results

The simulation results and A comparison between the simulation results and the actual results are shown in the following figures.

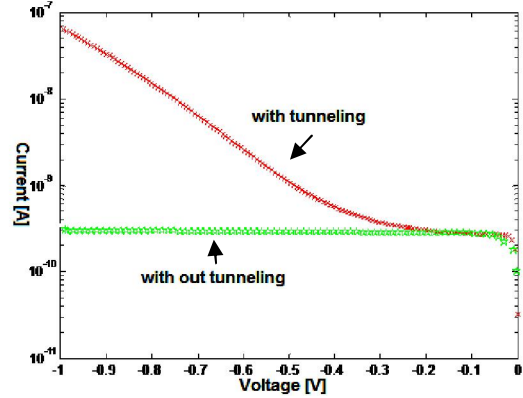


Figure 3: Dark current with and without tunneling model.

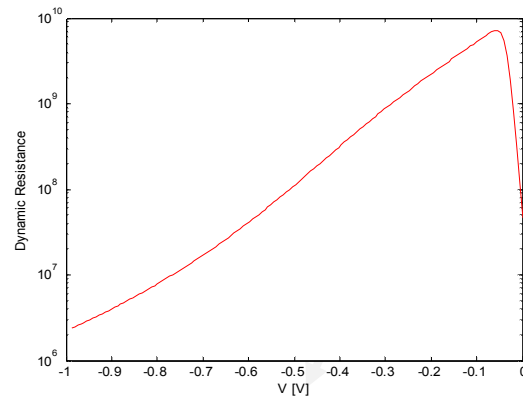


Figure 4: Dynamics of Resistance against reverse voltage.

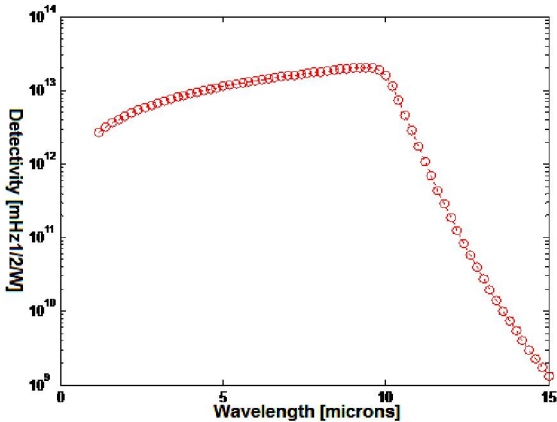


Figure 5: Detection versus wavelength.

Table 2 shows The simulation results compared with actual values.

First, a $p^+ - n$ junction of $Hg_{1-x}Cd_xTe$ with $x=0.225$ and $N_a = 2 \times 10^{17} cm^{-3}$, $N_d = 5 \times 10^{15} cm^{-3}$ At 77K Has been studied.

Table 2: Simulation results compared with actual values.

Desired quantity	Explanation	The simulation results	Analytical results
1.04/1.38	1.05	Energy Gap	E_g (e.V)
9/11.9	10.6	Cut-off wavelength	λ_{co} (μm)
8.1/10,5	9	The wavelength of maximum	λ_p (μm)
3×10^3	$10^3 \times 2.6$	Absorption coefficient	α (cm^{-1})
0.7	0.75	Quantum efficiency	η
7.5×10^{10}	8×10^{10}	Dynamic resistance	R_{QA}
8×10^{12}	10^{13}	Detection	D

As can be seen in Figure 6, the simulation results with the actual results are near appropriate and over estimates the performance of the device is. The difference between the results at the voltage closer to zero in comparison to more negative voltages is less, and its cause the modeling of tunneling.

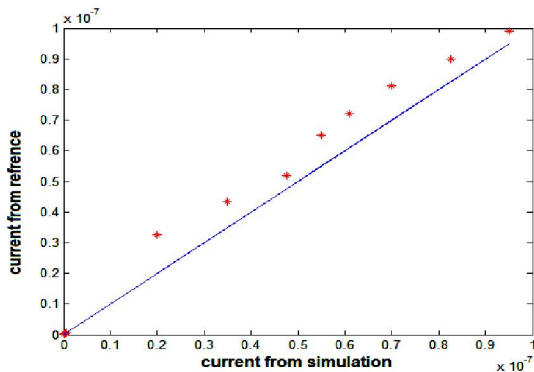


Figure 6: Comparison between the simulated and the current reference

As can be seen in Figure 3, Models with and without tunneling at negative voltages close to zero indicate better together, of course reasons of these difference are ionization and other computational errors such as rounding error and truncation error.

Correspondence to:

Electrical Department of Engineering Faculty, Shahid Chamran University, Ahwaz, Iran
Emails B-Boroomand@mststu.scu.ir

8/15/2013

References

- [1] A. Krier, "Mid-infrared Semiconductor Optoelectronics", Springer Series in Optical Sciences, pp. 3-8, 2006.
- [2] H. Kroemer, "The Einstein relation for degenerate carrier concentrations", IEEE Trans. Elec. Devices, vol. 25, No. 7, pp. 850, July 1978.
- [3] V. Srivastav, R.Pal, V. Venkataraman, "Performance study of high operating temperature HgCdTe mid wave infrared detector through numerical modelling", J. Appl. Phys. 108, 073112, 2010
- [4] B. Li, J.H. Chu, Y. Chang, Y.S. Gui, and D.Y. Tang, "Optical absorption above the energy band gap in Hg_{1-x}Cd_xTe", Infrared Phys. 32,195, 1991.
- [5] A. M Itsuno, J.D Phillips, S. Velicu, "Predicted performance improvement of Auger suppressed HgCdTe photodiodes and heterojunction detectors", IEEE Trans. Elec. Devices, vol.58, no.2, pp. 501-507, 2011.
- [6] K. Jozwikowski, M Kopytko, A. Rogalski, A. Jozwikowska, "Enhanced numerical analysis of current – voltage characteristics of long wavelength infrared n-on-p HgCdTe photodiodes", J. Appl. Phys., vol. 108, no. 7, 2010.
- [7] G.A.M Hurkx, D.B.M Klassen, M.P.G Knuvers, F.G O'Hara, "A new recombination model describing heavy .Int. Elec. Device Meeting, pp. 307-310, 1989.